

## Lattice Modelling of the Onset of Concrete-Ice Abrasion

Ramos, Nathalie; Shamsutdinova, G.; Hendriks, Max; Jacobsen, S.

**Publication date**

2016

**Document Version**

Accepted author manuscript

**Published in**

Concrete under Severe Conditions - Environment and Loading

**Citation (APA)**

Ramos, N., Shamsutdinova, G., Hendriks, M., & Jacobsen, S. (2016). Lattice Modelling of the Onset of Concrete-Ice Abrasion. In M. Colombo, & M. di Prisco (Eds.), *Concrete under Severe Conditions - Environment and Loading: Proceedings of the 8th International Conference on Concrete Under Severe Conditions - CONSEC2016* (pp. 351-358). Trans Tech Publications.

**Important note**

To cite this publication, please use the final published version (if applicable).  
Please check the document version above.

**Copyright**

Other than for strictly personal use, it is not permitted to download, forward or distribute the text or part of it, without the consent of the author(s) and/or copyright holder(s), unless the work is under an open content license such as Creative Commons.

**Takedown policy**

Please contact us and provide details if you believe this document breaches copyrights.  
We will remove access to the work immediately and investigate your claim.

# Lattice Modelling of the Onset of Concrete-Ice Abrasion

Nathalie Ramos<sup>1,a</sup>, Guzel Shamsutdinova<sup>2,b\*</sup>, Max A.N. Hendriks<sup>1,2,c</sup> and Stefan Jacobsen<sup>2,d</sup>

<sup>1</sup>Delft University of Technology, Delft, Netherlands

<sup>2</sup>Norwegian University of Science and Technology, Trondheim, Norway

<sup>a</sup>nathalieramos92@hotmail.com, <sup>b</sup>guzel.shamsutdinova@ntnu.no, <sup>c</sup>Max.Hendriks@ntnu.no,

<sup>d</sup>stefan.jacobsen@ntnu.no

**Keywords:** Lattice Modelling, concrete, ice, abrasion.

**Abstract.** The last decades the concrete-ice abrasion process has been well known as a concrete surface degradation mechanism due to ice sliding. The topic is especially relevant for concrete gravity based structures in the Arctic offshore.

The article presents a numerical model in which the onset of wear in the concrete-ice abrasion process is simulated. The simulations are performed on meso-scale, which means that concrete is modelled as a three-phase material in which paste, aggregates and the interface transition zone are distinguished. Lattice modelling is adopted for the numerical modeling. Hertzian contact theory which predicts excessive tensile stresses on the concrete surface due to sliding of ice asperities is used as an analytical basis for the numerical model. It was concluded that such model is able to capture both surface and subsurface cracking in the concrete.

## Introduction

Concrete-ice abrasion is a form of wear of concrete surfaces due to moving ice that has received attention during the last 2 – 3 decades, including experimental and theoretical research. Progress has been made lately to understand how the softer ice can wear the harder concrete [1].

So far, the assessment of concrete ice abrasion durability has mainly been evaluated experimentally, whereas less work has been done to model the actual degradation process. Laboratory measurements of concrete-ice abrasion are usually performed by concrete sliding on ice, see for example [2,3] or by ice sliding on concrete, see for example [4,5].

In this paper we present a study on the ongoing development of a FEA-model to understand the effect of variations in material-, surface- and load parameters of concrete and ice on resulting concrete ice abrasion. The current model is based on lattice modelling [6,7].

## Modeling steps

The numerical modelling of concrete-ice abrasion is far from straight forward. It involves ice mechanics, concrete mechanics and contact mechanics at various length scales. Moreover, the precise underlying mechanisms are still subject to debate. For these reasons, the development of numerical modelling is still in its exploratory phase. In the present paper the emphasis on a *possible* modeling approach by highlighting and distinguishing various modelling steps.

**From experiment to meso-scale.** The magnitude of the concrete-ice abrasion on structures can be in the order of 0.1 – 1 mm per year, whereas in the lab we typically produce wear in the order of 0.01 – 1 mm depth per km horizontal ice movement, depending on the concrete (strength, surface quality, etc.) and loading (ice properties, contact stress, temperature, etc.).

This numerical study is related to laboratory experiments performed with the equipment available at NTNU, Department of structural engineering [5]. At the NTNU lab concrete samples for laboratory experiments are rectangular in shape, 100 by 300 mm<sup>2</sup>, with height 50 mm. A cylindrical sample of

ice with diameter 73.4 mm slides along the upper horizontal concrete surface with a typical average pressure of 1 MPa (Fig. 1).

The numerical modelling steps take the laboratory experiments at NTNU as point of departure. First, it is assumed that the contact region consists of zones with a radius 10 mm. The size of 10 mm equals an assumed size of ice crystals [8]. Assuming an optimal packing of circular zones, this leads to 41 zones, Fig. 2(a). Next, it is assumed that some of the contact zones are flat and others are spherical, as indicated also in Fig. 2(a). It has been reported that approximately 10% of apparent ice area has a contact with the structure, during ice-structure interaction [9]. In general, tribology assumes this value to be below 20% [10]. By distinguishing flat and spherical contact zones, we ensured that 20% of apparent ice area has a contact with the concrete surface. Figure 2(b) shows a spherical contact zone, loaded by a force  $P$  which will depend on compressive strength of the ice. The modelling will zoom in on such contact zone for further studying concrete ice asperity interaction.

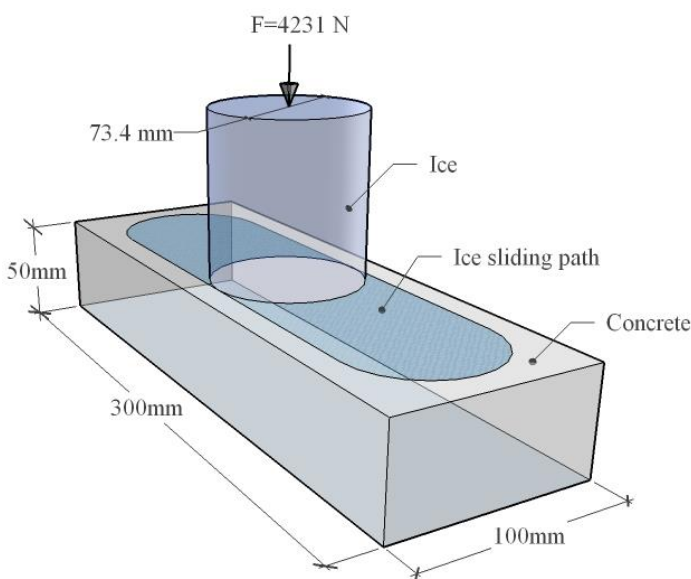


Figure 1. Scheme of the laboratory test

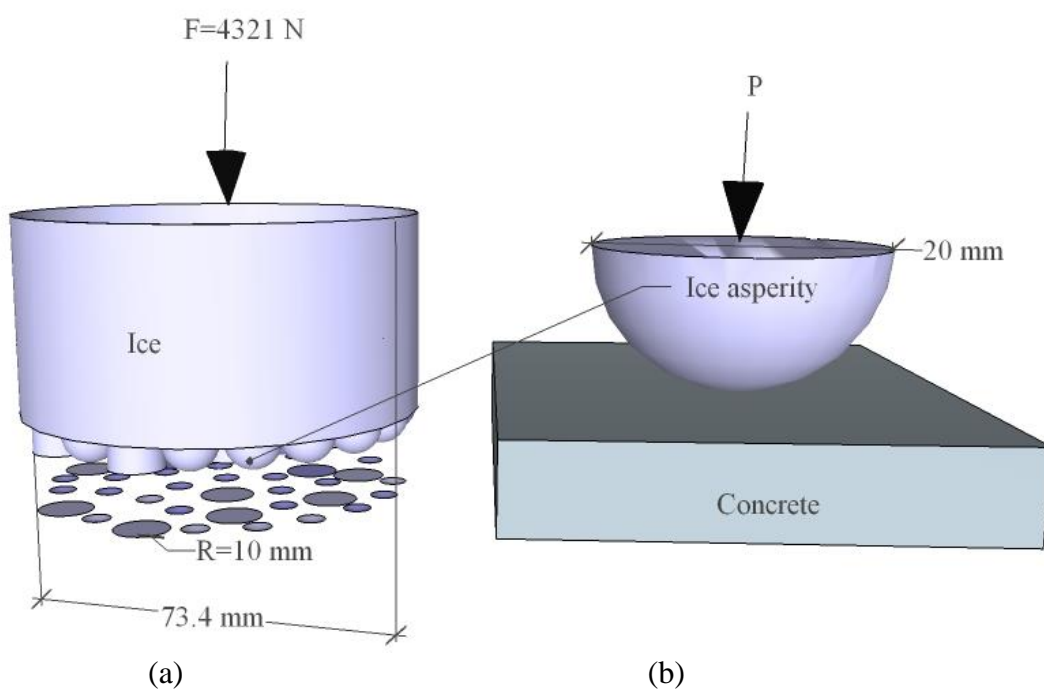


Figure 2. a) Schematic representation of non-homogeneous contact area; b) Ice asperity and concrete interaction

**Analytical solution for the contact area.** The analytical solution following from Hertz theory [11] is used to estimate the contact area and the local pressure profile between an ice asperity and the concrete surface. In a next step this analytical result will be used to uncouple the contact problem by assuming a load on the concrete. It is noted that the onset of wear in concrete-ice abrasion is a result of multiple mechanisms, which means that using the analytical solution according to Hertz can only provide insight to a certain or limited extent.

Hertzian contact theory, of the interaction between a half sphere and flat surface is adopted. Both materials, concrete and ice, are assumed to be elastic, homogeneous and isotropic. The deformation of the asperity, i.e. the radius of the contact area is calculated as, [11]

$$a = \left( \frac{3PR}{4E^*} \right)^{1/3} \quad (1)$$

where  $R$  is the radius of the ice crystal,  $P$  the load compressing the solids and  $E^*$  denotes the reduced modulus that depends on the Poisson's ratios and Young's moduli of both ice and concrete [11]. The ice load compressing the solids,  $P$ , is limited by the compressive strength of the ice,  $f_{c,ice}$ , per contact area [1], so that (Eq. 1) rewritten

$$a \leq \frac{3\pi R f_{c,ice}}{4E^*} \quad (2)$$

For a compressive strength of the ice of 50 MPa, the radius of the contact area is equal to 64.8  $\mu\text{m}$  (Fig. 3). According to the Hertzian theory, the pressure at the center of the contact circle,  $p_0$ , is 50% larger than the average pressure on the asperity (Eq. 3). It is assumed that the average pressure is restricted by the physical limit of the ice which is equal to ice compressive strength,  $f_{c,ice}$

$$p_0 = \frac{3}{2} f_{c,ice} \quad (3)$$

This gives a maximum pressure at the center of the contact circle. Further distribution of normal pressure is given by Hertz theory as a function of the contact radius (Eq. 4), with the assumption that we neglect any interaction between normal pressure and tangential traction arising from a difference in elastic constants of the two solids [14]. The tangential traction is derived according to the law of dry friction (Eq. 5).

$$p(r) = p_0(1 - (r/a)^2)^{1/2} \quad (4)$$

$$q(r) = \mu p_0(1 - (r/a)^2)^{1/2} \quad (5)$$

**Decoupling the contact interaction.** From here on the contact interaction between concrete and ice is decoupled. This means that the two materials are modelled separately. It is assumed that the contact conditions, like contact area and contact pressure, are preserved through Hertz contact theory. The modeling is now focused on the concrete with an assumed pressure profile, (Fig. 4a).

**2D representation.** 2D representation. Fig. 4 also illustrates a subsequent modelling step; the 3D contact problem is simplified to allow the 2D modelling of a thin slice of 20  $\mu\text{m}$ . A 2D plane stress state is assumed. The appropriateness of this assumption is clearly subject for debate. The nodal equivalent forces in the contact area have been calculated. Even though a thin slice of concrete is modelled, the width of the entire contact area is used to calculate the nodal equivalent forces.

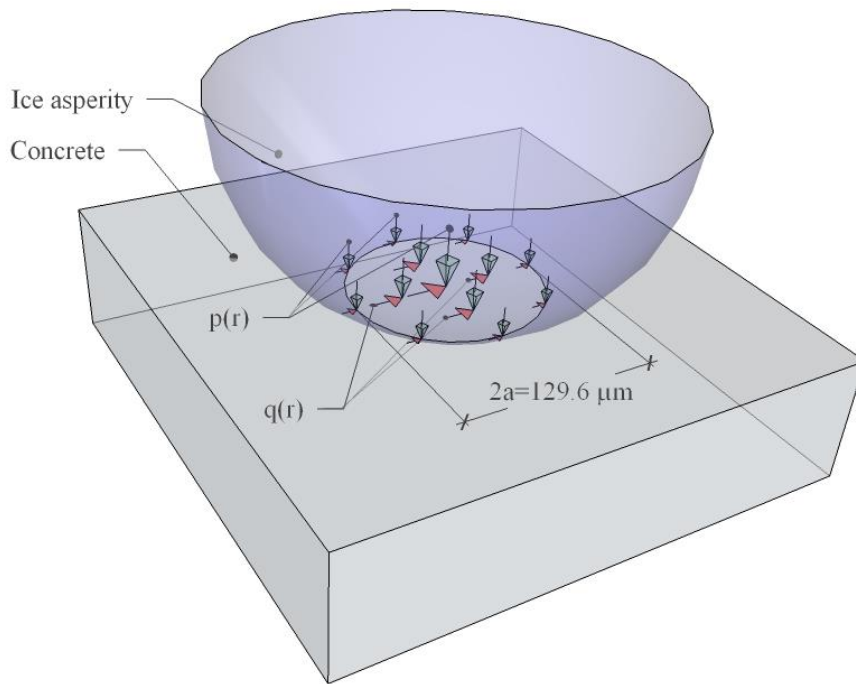


Figure 3. Scheme of pressure distribution on a contact zone.

A 2D regular lattice model ... A 2D regular lattice model is used. The contact pressure is discretized into nodal equivalent forces, (Fig. 4b). The size of the lattice elements is set to  $20\ \mu\text{m}$ . This allows for a reasonable approximation of the contact stress distribution in the discretized model. A 2D slice of the concrete sample of  $2 \times 2\ \text{mm}^2$  is modeled. The selected element length of  $20\ \mu\text{m}$  leads to manageable computation times.

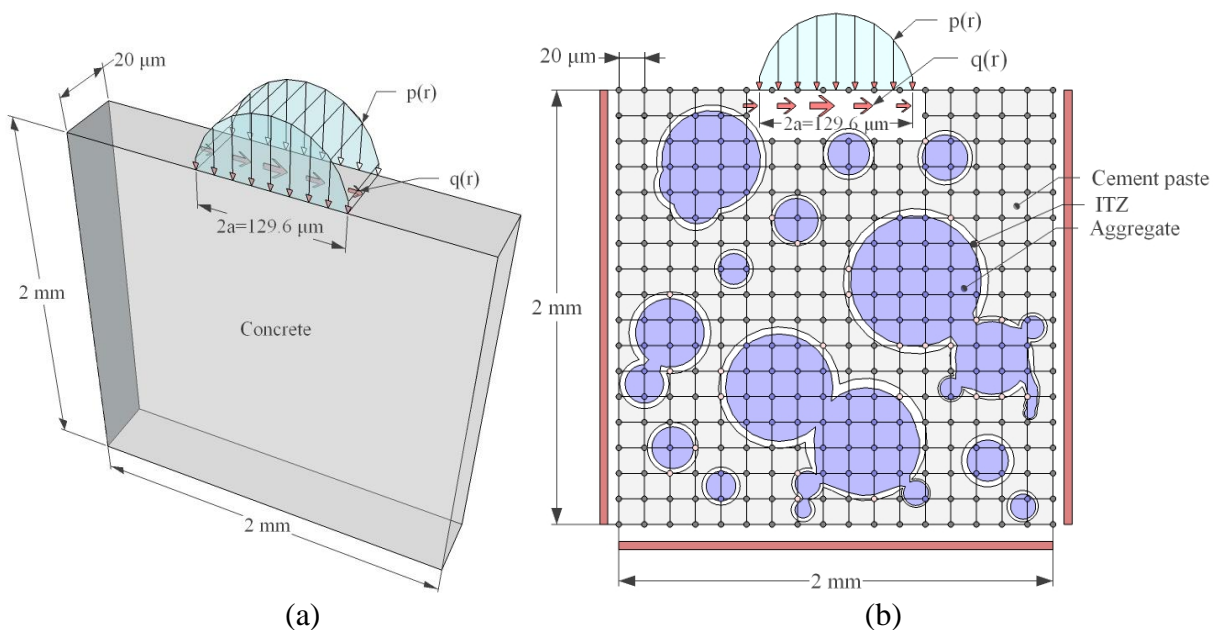


Figure 4. a) Schematic slice of 3D contact problem; b) 2D model with simply supported edges. Figures at not at scale: the extend of the concrete region is larger in the model.

**Boundary conditions.** Hertz theory assumes that the radius of the contact area is small compared to the radius of the asperity. It also assumes that the contact behavior occurs very locally and is not influenced by edges. The *simply supported edges* are applied in the numerical simulations (Fig. 4(b)).

**Materials.** Since the numerical study is related to laboratory experiments, the properties of concrete were chosen as B60 and B70, which are often used in the experiments. All simulations, besides one, have been modeled with inhomogeneous properties for the concrete. For the inhomogeneous models three phases of concrete are distinguished: cement paste, ITZ (interfacial transition zone) and aggregates. The elastic properties of B60 and B70 concrete are summarized in Table 1. The grain size distribution of aggregates within the slice of concrete was taken from the lower part of typical 0/8 mm sand with a volume fraction of 50% in the concrete. The properties of ice are a the compressive strength,  $f_{c,ice} = 50$  MP and modulus of elasticity,  $E_{ice} = 10 \cdot 10^3$  MPa.

Table 1. Elastic properties of B60 and B70

Component	E [MPa]	$f_t$ [MPa]	$f_c$ [MPa]
B60			
Cement paste	43000	7.5	-74.4
ITZ	21500	3.7	-74.4
Aggregates	50000	14	-200
B70			
Cement paste	50500	10.2	-102.2
ITZ	25300	5.1	-102.2
Aggregates	50000	14	-200

## Results and discussion

A few analysis results are presented and discussed shortly in the sequel.

**Homogeneous versus heterogeneous modeling of concrete.** Cracking in the homogeneous and heterogeneous model shows significant differences, (Fig. 5). The only cracks which occur in the homogeneous model, are small surface cracks at the front and back edge of the contact. The heterogeneous model shows some significant cracking, which are mainly localized along the ITZ. Subsurface cracking turns out to be more significant in magnitude than surface cracking.

**Influence of friction coefficient.** The coefficient of friction influences the load at which surface damage occurs. For an increasing coefficient of friction, the surface cracks arise at a lower load (Fig. 6):

- $\mu=0.05$ : surface crack initiation at load step 100 ~ 67 % of loading;
- $\mu=0.1$ : surface crack initiation at load step 50 ~ 50 % of loading;
- $\mu=0.2$ : surface crack initiation at load step 20 ~ 15 % of loading.

**Concrete quality.** Figure 7 shows the final crack patterns for the cases with B70 and B60 concrete. A similar crack pattern is observed. For the B60 concrete a more pronounced subsurface cracking is observed.

**Roughness.** Since the concrete surface is not perfectly smooth as was assumed above, the next simulation cases explore the concrete surface roughness effect. As a reference, the smooth surface model for B60 is considered. Figure 8 shows the damage evaluation for three subsequent loading steps. Next a simplified surface roughness is considered by assuming rectangular grooves. The grooves have a width of 0.3 mm and a depth of 0.06 and 0.1 mm for *Profile 1* and *2* respectively. The cracking mechanism for the rough model with roughness profile 1, Figure 9, is similar to that of the smooth model; subsurface cracks propagate through the cement paste and along ITZ's. The subsurface crack profile is similar to the crack profile of the smooth model. Differences are apparent when the cracks reach the surface. Also the subsurface cracking pattern of *profile 2*, Figure 10, coincides well with the subsurface cracking patterns found in both the smooth model and in the rough model with surface *profile 1*. Apparently, the depth of the adopted grooves is insufficient to cause significant deviations in the subsurface cracking behavior.

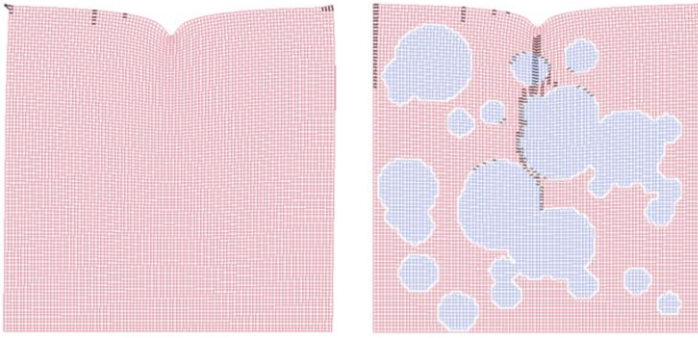


Figure 5. (a) Crack pattern homogeneous model, (b) Crack pattern heterogeneous model (both during the final load step)

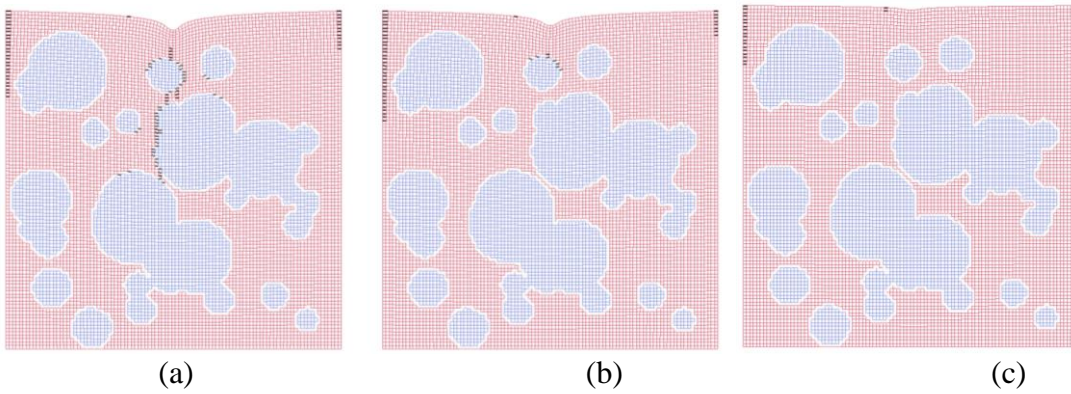


Figure 6. (a) Crack pattern for  $\mu=0.05$  at load step 100, (b) Crack pattern for  $\mu=0.1$  at load step 50, (c) Crack pattern for  $\mu=0.2$  at load step 20

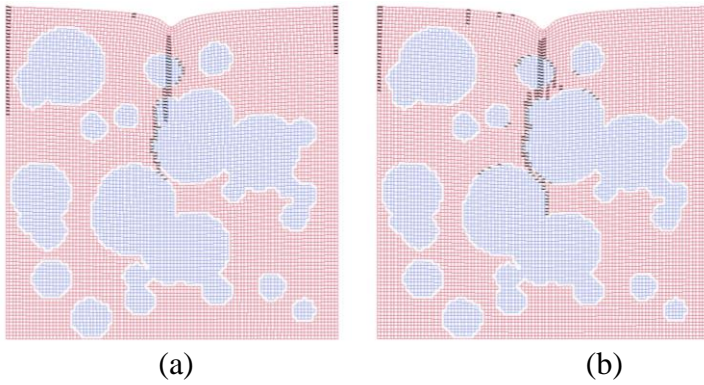


Figure 7. (a) Cracking pattern B70 concrete, (b) Cracking pattern B60 concrete (both during final load step)

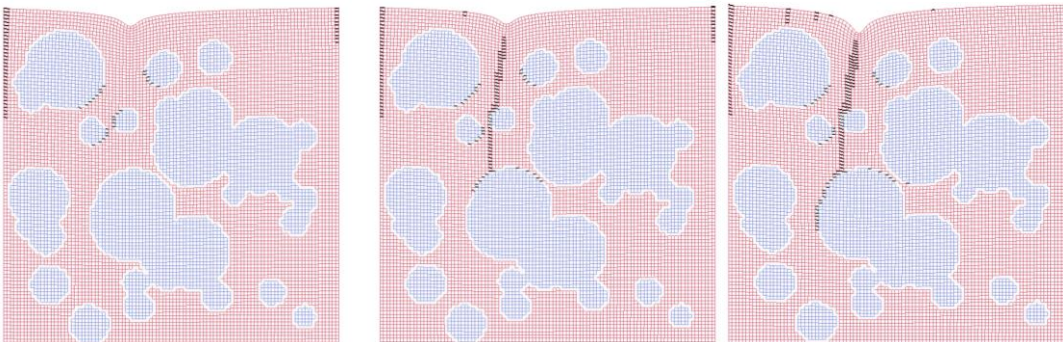


Figure 8. Crack patterns of the default smooth model as the loading increases

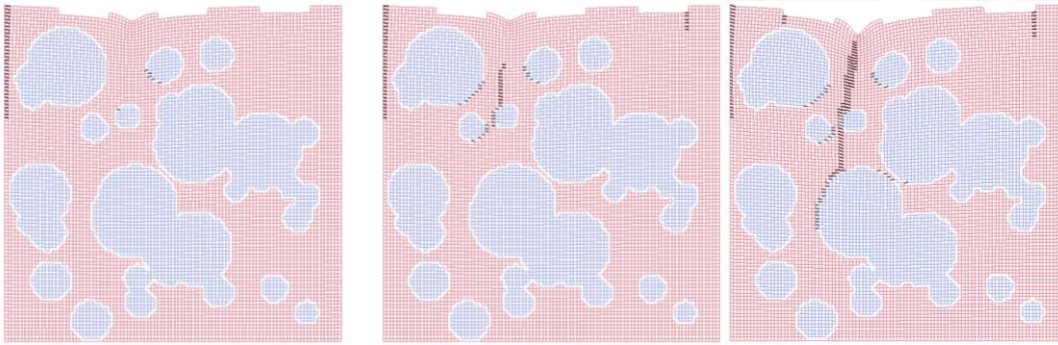


Figure 9. Crack patterns of the model with surface profile 1 as the loading increases

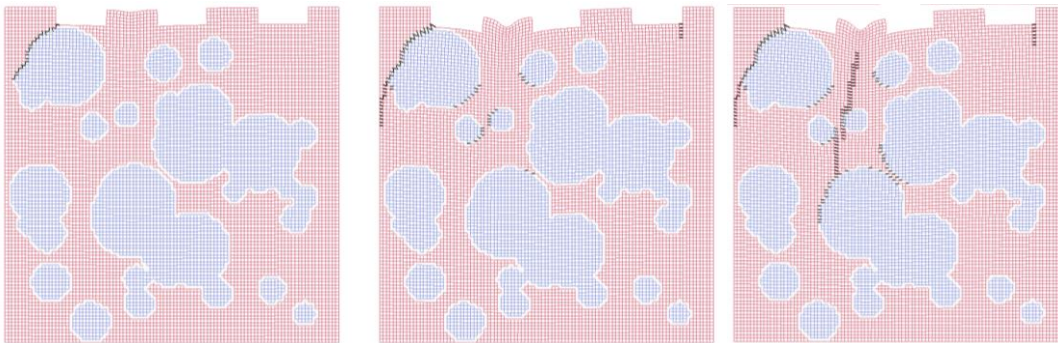


Figure 10. Crack patterns of the model with surface profile 2 as the loading increases

## Conclusion

It can be concluded that a numerical model that simulates (sliding) contact between concrete and ice, can potentially be used to model the onset of wear during the concrete-ice abrasion process. The current model focusses on the scale of tens of  $\mu\text{m}$ . Both the loading distribution caused by ice asperities and the inhomogeneity in the concrete were considered at this scale. Many modeling steps were required to come to the current model. Many of these steps we were not explicitly verified. It is even unclear which of the modelling steps are critical. This illustrates the exploratory character of the current modelling stage. With this in mind, some preliminary conclusions could be drawn.

- The inhomogeneous models reveal subsurface cracking. A homogeneous model for concrete is unable to capture subsurface cracking.
- The model captures surface cracks even when the reduced properties of the ITZ of the concrete are not taken into account.
- The model provides insight in the (relative) magnitude of cracking and the order of cracking in various concretes, under various loading conditions.
- The current model does not provide information on the influence of surface roughness.

Further development of the numerical modeling is envisioned. Various improvements will be considered including:

- The basic assumption of the load transmission through the ice at the scale of mm and  $\mu\text{m}$ ;
- The justification of quantification of real versus apparent contact areas;
- The quantification of the compressive strength of ice at the scale of mm;
- The impact of full 3D modelling.
- The appropriateness of the used discretization method.

## References

- [1] S. Jacobsen, G. W. Scherer and E. M. Schulson, Concrete-Ice Abrasion Mechanics, Cement and Concrete Research, 73 (2015) 79–95



- [2] Y. Itoh, A. Yoshida, M. Tsuchiya, K. Katoh, K. Sasaki and H. Saeki, An experimental study on abrasion of concrete due to sea ice, Presented at the 20th Annual Offshore Technology Conference in Houston, Texas, May 2–5 (1988) 61–68
- [3] A.T. Bekker, T.E. Uvarova, E.E. Pomnikov, A.E. Farafonov, I.G. Prytkov and R.S. Tyutrin, Experimental Study of Concrete Resistance to Ice Abrasion. Proceedings of the 21-th Int. Offshore and Polar Engineering Conference, Maui, Hawaii, USA, June 19-24 (2011) 1044-1047.
- [4] A. M. Nawwar and V. M. Malhotra, Development of a Test Method to Determine the Resistance of Concrete to Ice Abrasion and/or Impact, American Concrete Institute SP 109 (1988) 401-426.
- [5] G. Shamsutdinova, P. B. Rike, M. A. Hendriks and S. Jacobsen, Concrete Ice Abrasion Rig and Wear Measurements, International Conference on Port and Ocean Engineering under Arctic Conditions, Trondheim, 23 (2015).
- [6] E. Schlangen and E.J. Garboczi, Fracture Simulations of Concrete Using Lattice Models: Computational Aspects, Engineering Fracture Mechanics 57 (2-3) (1997) 319-332.
- [7] G. Lilliu and J. G. van Mier, On The Relative Use of Micro-Mechanical Lattice Analysis of 3-Phase Particle Composites, Engineering Fracture Mechanics 74 (7) (2007) 1174-1189.
- [8] P. V. Hoobbs, Ice Physics, Oxford University Press (2010) 668.
- [9] R. Taylor, R. Frederking and I. Jordan, The Nature of High Pressure Zones in Compressive Ice Failure, The 19th International Symposium on Ice, Vancouver, (2008) 1001-1010.
- [10] B. Basu and M. Kalin, Tribology of Ceramics and Composites. A material Science Perspective, New Jersey, 2011.
- [11] K. Jonson, Contact Mechanics, London, 1985.